Electron-spin-resonance studies of pristine and heavily doped polyacenic materials

Kazuyoshi Tanaka, Tsuneaki Koike, and Tokio Yamabe
Department of Hydrocarbon Chemistry and Division of Molecular Engineering, Faculty of Engineering, Kyoto University, Sakyo-ku, Kyoto 606, Japan

Jun Yamauchi and Yasuo Deguchi
College of Liberal Arts and Sciences, Kyoto University, Sakyo-ku, Kyoto 606, Japan

Shizukuni Yata
Development Laboratories, Kanebo Ltd., Miyakojima-ku, Osaka 534, Japan
(Received 5 November 1986)

Electron-spin-resonance (ESR) studies of pristine and heavily doped polyacenic materials prepared by pyrolytic treatment of phenolformaldehyde resin have been carried out. Five pyrolysis temperatures (T_p) in the range 500–900 °C were selected to check the magnetic properties of the samples. The ESR line shapes and the spin concentrations of the pristine samples strongly depend on T_p, reflecting the structural characteristics in each sample. The ESR measurement of the doped samples, along with the electrical transport study previously reported, leads to the picture that both the *p*-type and the *n*-type dopants (I_2 and Na) essentially have two kinds of roles: (i) scavenging of the magnetic impurities, the energy levels of which exist near the Fermi level, and (ii) generation of conduction carriers giving broadened ESR spectra, particularly in the samples prepared at higher T_p. From this observation, it is highly possible that in such doped samples, the spin-orbit coupling plays an important role in the relaxation process, which suggests that the conduction carriers exist on the dopant species with a finite probability.

I. INTRODUCTION

It is well known that amorphous (glassy) carbon compounds prepared by pyrolytic treatment of organic materials are semiconductive their electric conductivity varying according to the applied pyrolysis temperature (T_p). Typical starting materials for these are phenolformaldehyde (PF) resin,[1,2] polyimides such as Kapton[3] or poly (*p*-phenylene-1,3,4-oxadiazole),[4] polyacrylonitrile,[5] and cellulose.[1,6] Recently we demonstrated for the first time that polyacenic semiconductive materials prepared by the pyrolysis of PF resin can be doped with both electron acceptors and donors resulting in an increase of the electrical conductivity by 11 orders of magnitude at maximum.[7] This class of material particularly seems to be promising in its application to electric and/or electronic devices because of its stability in air and tractability of preparation.[8]

It is understood that the structure of this polyacenic material is an incomplete version of graphite consisting of carbonized or "graphitized" fractions. Electrical transport studies have shown that the conduction mechanism in this material is explained by three-dimensional variable-range hopping (3D VRH) for the lower-T_p ($\sim$600 °C) sample.[9] Furthermore, in the higher-T_p ($\sim$900 °C) sample, the mechanism was concluded to be a mixed version of nearly filled-band metallic features together with hopping processes, which suggests the existence of metallic islands therein.[9] X-ray diffraction analyses of the series of these samples also supported the picture of disordered structures with hard-graphitizing characteristics.[10]

In an earlier paper,[11] a preliminary ESR study on the current material in its pristine state indicated the existence of radical spins of π nature as a sort of magnetic impurity dependent upon the degree of the development of the graphitized network or the polyacenic skeletons. Similar magnetic impurities were also reported in other pyrolytic carbons starting from miscellaneous polymers.[6]

Energy levels of these radical spins should exist between the conduction and the valence bands;[12] that is, near the Fermi level, and hence are expected to be extremely sensitive to doping. Furthermore, as the doping proceeds, it is possible that conduction carriers will appear in the metallic-island region. In these respects, it is of obvious interest to analyze the changes in magnetic properties of the present polyacenic materials upon the doping procedure based on ESR spectroscopy.

In this article, we report and discuss the results of ESR spectroscopic studies of pristine and heavily doped polyacenic materials. Five T_p's in the range 500–900 °C were selected for pyrolytic treatment of PF resin in the present study in order to check the difference in magnetic properties. Both the *p*-type and the *n*-type dopings of all of these pristine samples were carried out using iodine and sodium, respectively, up to the saturation limit of the electrical conductivity of each sample.

II. EXPERIMENTAL

A. Sample preparation

The pristine samples were prepared by pyrolysis of molded PF resin. The pyrolytic procedure was performed

TABLE I. Pyrolysis temperature (T_p in °C), [H]/[C] molar ratio, electrical conductivity at room temperature (σ in S cm^{-1}), $\Delta H_{1/2}/\Delta H_{\text{p.p.}}$, peak-to-peak linewidth ($\Delta H_{\text{p.p.}}$ in G), spin concentration (N_s in spins/g), carbon number per spin (N_c), and g value of the samples. Values in parentheses are those measured at −100 °C.

Sample	T_p	[H]/[C]	σ	$\Delta H_{1/2}/\Delta H_{\text{p.p.}}$	$\Delta H_{\text{p.p.}}$	N_s	N_c	g value
*A*1	525	0.44	1.5×10^{-13}	2.47	5.96	5.1×10^{19}	945	2.0026
				(2.43)	(6.62)	(5.0×10^{19})	(976)	(2.0023)
B	585	0.37	4.9×10^{-10}	2.74	2.52	6.1×10^{19}	799	2.0025
				(2.96)	(2.34)	(9.0×10^{19})	(544)	(2.0021)
D	680	0.24	7.0×10^{-5}	2.82	0.31	1.2×10^{20}	407	2.0024
				(3.00)	(0.43)	(2.3×10^{21})	(28)	(2.0025)
E	775	0.15	5.0×10^{-2}	2.33	2.78	8.8×10^{19}	565	2.0022
				(3.13)	(1.32)	(1.3×10^{20})	(382)	(2.0022)
G	865	0.08	5.9×10^{0}	2.64	8.48	2.2×10^{19}	2257	2.0027
				(2.82)	(7.04)	(3.9×10^{19})	(1265)	(2.0022)

in a non-oxidative atmosphere. The chemistry involved in this pyrolytic treatment was discussed in the earlier publication.[7] In the present experiment, samples were made to have a fibrous structure in order to achieve a uniform diffusion of dopants. Details of prescription of the sample preparation are described elsewhere.[9,13]

Five pristine samples, labeled *A*1, *B*, *D*, *E*, and *G* were prepared under accurate temperature control in the range 525–865 °C. These samples were also used as the starting material for the doping process. Each sample was made into the form of a plate (about 1.5×1.5 cm^2 or less) with thickness of 800–1100 μm. They appear as dull black-colored solids due to their fibrous structure, and are insoluble and infusible. In the second and the third columns of Table I are listed the T_p and the [H]/[C] molar ratios of the pristine samples determined from the elemental analyses. The latter values indicate the degree of carbonization. The electrical conductivity of all the samples at room temperature was measured *in vacuo* by the combination of two-probe (for $\sigma<10^{-5}$ S cm^{-1}) and four-probe techniques.

Iodine and sodium dopings were carried out by the conventional techniques employed in Ref. 7 until the increase of the electrical conductivity saturated. The [I]/[C] molar ratios in Table II were determined by elemental analyses, whereas the [Na]/[C] values in Table III were determined by titration of sodium ions after a thorough undoping of sodium from the doped sample into water.

B. ESR measurement

Each sample was milled into fine powder to prevent a skin effect. For instance, the skin depth of the sample given by

$$\delta=(\pi\nu\sigma)^{-1/2}$$

becomes approximately 0.02 cm for the combination of $\sigma=1\times10^{1}$ S cm^{-1} and the electromagnetic frequency, $\nu=9$ GHz. The powdered sample was then sealed in a 4.75-mm-outer-diameter quartz tube for the ESR measurements after evacuation down to less than 10^{-4} Torr for 5 h maximum in order to remove the absorbed oxygen that possibly acts as a dopant.[11] In particular, the sodium-doped samples were treated under N_2 atmosphere to protect sodium from reacting with moisture in air and then sealed in the ESR tube after evacuation.

All of the ESR measurements were performed with a JEOL JES-FE3X ESR Spectrometer at *X* band (9.4 GHz). The microwave power was fixed well below (about 10%

TABLE II. Results for the iodine-doped samples. Headings are the same as in Table I.

Sample	[I]/[C]	σ	$\Delta H_{1/2}/\Delta H_{\text{p.p.}}$	$\Delta H_{\text{p.p.}}$	N_s	N_c	g value
I_2-*A*1	0.07	2.6×10^{-5}	2.89	7.87	1.0×10^{20}	274	2.0043
			(2.35)	(9.26)	(7.9×10^{19})	(358)	(2.0044)
I_2-*B*	0.07	1.7×10^{-3}	2.67	20.12	6.2×10^{19}	458	2.0042
			(2.59)	(11.35)	(1.2×10^{20})	(230)	(2.0042)
I_2-*D*	0.07	1.4×10^{-1}	2.09	83.04	1.6×10^{20}	177	2.0080
			(2.55)	(42.98)	( )[a]	( )[a]	(2.0051)
I_2-*E*	0.07	2.6×10^{0}	2.40	229.84	1.9×10^{20}	154	2.0055
			(2.47)	(127.86)	(2.4×10^{20})	(119)	(2.0027)
I_2-*G*	0.06	3.7×10^{1}	2.68	699.03	b	b	2.1191
			(2.62)	(≈560)	( )[b]	( )[b]	( )[b]

[a]Both DPPH and $CuSO_4\cdot5H_2O$ standards were not applicable.
[b]Impossible to measure.

TABLE III. Results for the sodium-doped samples. Headings are the same as in Table I.

Sample	[Na]/[C]	σ	$\Delta H_{1/2}/\Delta H_{p.p.}$	$\Delta H_{p.p.}$	N_s	N_c	g value
Na-*A*1	0.04	9.3×10^{-7}	2.34	6.36	2.6×10^{19}	1704	2.0032
			(2.13)	(7.63)	(2.8×10^{19})	(1593)	(2.0029)
Na-*B*	0.03	3.6×10^{-3}	2.43	1.01	2.1×10^{19}	2174	2.0026
			(2.75)	(1.73)	(7.3×10^{19})	(632)	(2.0030)
Na-*D*	0.08	9.4×10^{-1}	2.81	1.86	1.3×10^{18}	32158	2.0029
			(2.78)	(1.14)	(2.1×10^{18})	(20318)	(2.0029)
Na-*E*	0.05	9.0×10^{0}	3.00	3.35	2.0×10^{18}	22327	2.0031
			(3.90)	(1.44)	(1.1×10^{19})	(4263)	(2.0028)
Na-*G*	0.06	3.7×10^{1}	2.65	12.83	1.5×10^{19}	2900	2.0023
			(2.97)	(11.26)	(6.7×10^{18})	(6515)	(2.0024)

of) the value causing signal saturation. The modulation width was kept at 25% of the peak-to-peak linewidth ($\Delta H_{p.p.}$; see Fig. 1) of each sample.

The data were obtained for the samples kept at room temperature and at $-100\,^{\circ}C$. A Mn^{2+}-MgO solid solution was used as a reference for the g value and the magnetic field calibration. Determination of the spin concentration was made by using $CuSO_4\cdot5H_2O$ and 1,1'-diphenyl-2-picrylhydrazyl (DPPH) as standards. The former had been purified by recrystallization from aqueous solution and calibrated by the latter obtained by recrystallization from chloroform solution and by successive purification with column chromatography using silica gel (Wakogel C-200). The $CuSO_4\cdot5H_2O$ standard was used for the peaks with $\Delta H_{p.p.}$ less than 50 G, whereas the DPPH standard diluted with silica gel (Wakogel C-300) down to a factor of 1.2×10^{-3} was employed for the peaks with $\Delta H_{p.p.}$ of more than 50 G. To check the line shape the ratio $\Delta H_{1/2}/\Delta H_{p.p.}$ of each peak (see Fig. 1) was calculated. Rigorous Gaussian and Lorentzian line shapes give the values 1.92 and 2.40, respectively, for this ratio.

III. RESULTS AND DISCUSSION

The results of the ESR measurements of the pristine and the heavily doped samples are listed in Tables I–III.

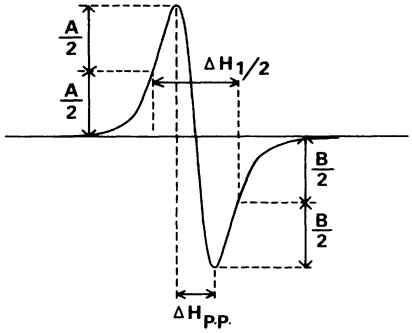

FIG. 1. Illustrative definition of $\Delta H_{p.p.}$ (peak-to-peak linewidth) and $\Delta H_{1/2}$ (outside half-height linewidth of the differential peak) of an ESR spectrum. For all the samples except I_2-*G* the line shape is symmetric ($A=B$).

The values in parentheses are those measured at $-100\,^{\circ}C$. The relative errors of the observed $\Delta H_{p.p.}$ and g values are less than 1.7% and 0.04%, respectively, except I_2-*G*. Because of the broad ESR line shape of I_2-*G*, the errors of $\Delta H_{p.p.}$ and g value of this sample are estimated to be within 4.2% and 0.1%, respectively. The maximum error inherent in the observed spin concentration (N_s) is estimated to be 5%. The ESR line shapes observed under room temperature are shown in Figs. 2(a)–(c). These are discussed stepwise in what follows.

A. Pristine samples

The ESR spectra of all the pristine samples in Fig. 2(a) consist of a single narrow line with no hyperfine splitting. The line shapes are nearly Lorentzian as indicated by the values of $\Delta H_{1/2}/\Delta H_{p.p.}$ in Table I. Regarding all the line

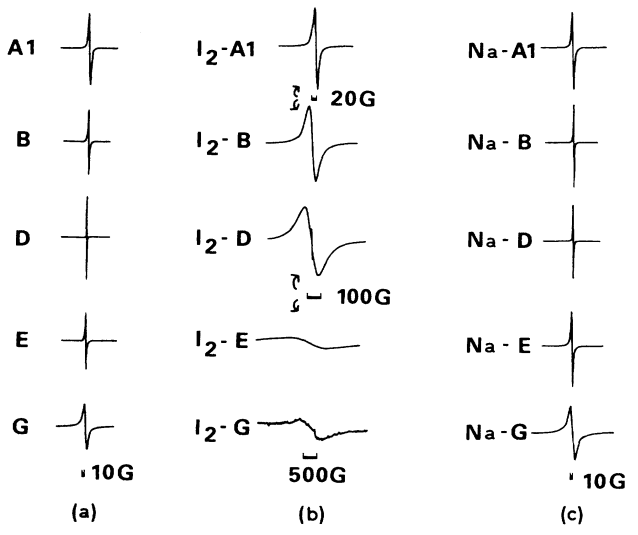

FIG. 2. ESR spectra of (a) the pristine, (b) the iodine-doped, and (c) the sodium-doped samples at room temperature. The amplitude for all the measurements except I_2-*D*, I_2-*E*, and I_2-*G*, was the order of $\times100$. For these three cases, the amplitude was the order of $\times1000$.

shapes as Lorentzian, the transverse (spin-spin) relaxation time,

$$T_2 = \frac{2}{\sqrt{3}\pi\Delta H_{\text{p.p.}}}$$

is calculated to be on the order of 10^{-8}–10^{-9} s for all the samples. The values of T_2 of *trans*-polyacetylene and graphite are, respectively, 7.8×10^{-8} s (Ref. 14) and 2.0×10^{-8} s (Ref. 15).

The value of $\Delta H_{\text{p.p.}}$ in Table I decreases from *A*1 to *D* and then increases in *E* and *G*. The spin concentration (N_s) or, equivalently, the number of carbons per spin (N_C) indicates that the number of unpaired electrons becomes maximum for *D*. This relationship is sketched in Fig. 3. The increase in $\Delta H_{\text{p.p.}}$, that is the broadening of the line in *E* and *G*, does not seem to be inhomogeneous broadening, since the line shapes are still Lorentzian. These observations lead to an interpretation that in the polyacenic sample with $T_p \sim 700$ °C (namely *D*) the spin concentration becomes maximum and the linewidth becomes minimum due to exchange narrowing. Similar behavior of these quantities depending on T_p was reported in earlier studies of pyrolized cellulose, vinyl polymers, and PF resin.[6,16]

Our previous report of the measurements of thermoelectric power and electrical conductivity of *E* and *G* showed that their structure contains metallic islands.[9] On the other hand, the 3D VRH mechanism is dominant in the samples with T_P lower than 600 °C.[9]

Synthesizing all the data available, we conclude that, in the present polyacenic samples with T_p lower than 700 °C, a number of graphitized fractions of small size are gradually formed with as T_p increases. These fractions are so small and/or incomplete that they cannot yet be defined as metallic islands. Hence the 3D VRH mechanism prevails in these materials. Such small graphitized fractions are supposed to have a number of dangling bonds consisting of unpaired electrons in their boundary region.

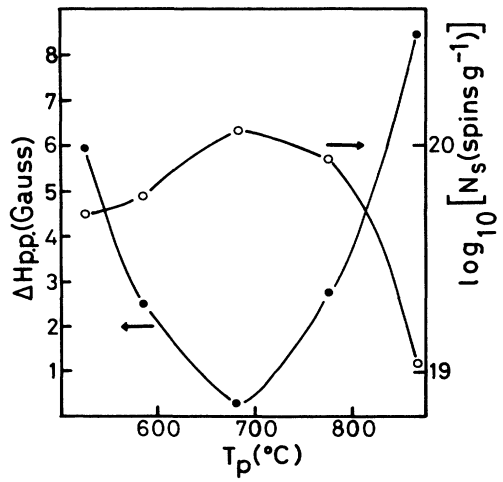

FIG. 3. Peak-to-peak linewidth $\Delta H_{\text{p.p.}}$ and spin concentration N_s vs T_p for the pristine samples. Solid lines are guides for the eye.

Therefore, an increase of T_p is accompanied by an increase of the spin concentrations. On the other hand, in the samples with T_p higher than 700 °C, growth of the above small fractions through nucleation or condensation begins to develop metallic islands, as is evident from the occurrence of a semiconductor-metal transition in *E* or *G* based on the thermoelectric power measurement.[9] At the same time, this process diminishes the spin concentration owing to the recombination and, hence, the annihilation of dangling bonds.

Even the samples with higher T_p's such as *E* and *G*, however, do not show the asymmetric ESR line shape (Dysonian) characteristic of a metallic material.[17] This indicates that the size of metallic islands in these samples is small compared with the skin depth (e.g., about 0.02 cm for $\sigma = 1\times10^{1}$ S cm^{-1}; see Sec. II B). This situation also holds in the iodine- and sodium-doped samples.

The dangling bond on a carbon atom in the boundary region of the metallic island originally occurs from the cleavage of the σ bonds of the carbon atom involved in the process of carbonization. Hence, in this sense, it may well be considered that the nature of spins observed is of σ type. It has been pointed out, however, that unpaired σ electrons (σ radicals) thus formed are energetically unstable compared with unpaired π electrons (π radicals) that can be delocalized possibly over a graphitized fraction.[18] Therefore, unpaired electrons of σ type will readily convert into π type becoming mobile and delocalized. In fact, all the pristine samples show a single narrow line shape with no hyperfine splittings of the ESR peak and have *g* values in the range 2.0021–2.0027 comparable with those of a free electron (2.0023) or π radicals in *trans*-polyacetylene (2.00263).[19] It is concluded that the unpaired electron species found in the present pristine samples are of π type, either directly or indirectly occurring from structural defects or kinks.

From Table I the results of the ESR measurement at −100 °C are not much different from those at room temperature. However, in *E* and *G*, an obvious narrowing of the line appears at −100 °C. This behavior may be explained by enhancement of the exchange interaction between spins at lower temperature due to a suppression of phonon vibrations or by a Korringa-type mechanism[20] for the longitudinal (spin-lattice) relaxation time T_1 and temperature *T*,

$$T_1 T = \text{const}$$

as has been invoked in the case of the iodine-doped polyacetylene.[21]

B. Iodine-doped samples

The results of the samples heavily doped with iodine are shown in Fig. 2(b) and Table II. The values of $\Delta H_{\text{p.p.}}$ of all the samples are larger than those of the pristine samples. Indeed, those of I_2-*D*, I_2-*E*, and I_2-*G* are considerably larger, the signal intensities being approximately $\frac{1}{10}$ of the pristine signal. It was confirmed by additional ESR measurements of the pristine samples with higher gains that these broad and weak ESR signals are not originally hidden in the foot of the sharp signal of the pristine sam-

ple concerned. Actually, we already reported based on the *in situ* doping technique during the ESR measurement that the sharp ESR signal of the pristine *E* and *G* samples disappears and then the broad peak appears with the progress of the doping by iodine (and bromine).[22]

Hence it is concluded that the broad ESR signals are inherent in the iodine-doped samples. Incidentally, in I_2-*D*, a typical two-phase spectrum is seen as in Fig. 2(b), indicating that the original unpaired electron species of the pristine structure still remain even after the heavy doping.

The spin concentrations of the I_2-doped samples are apparently larger than those of the pristine sample as listed in Table II. However, the above mentioned *in situ* doping experiment[22] suggests that this quantity decreases at the initial stage of the doping and then continues to increase until the heavily doped stage. The defect-oriented unpaired electrons mostly accommodated in the impurity levels near the Fermi level of the pristine sample are scavenged at the initial stage of the doping by iodine which is an electron acceptor, leaving holes in these impurity levels. In the heavily-doped stage, more holes are generated by iodine near the top of the valence band as illustrated in Fig. 4 and play the role of *p*-type conduction carriers.

Broad ESR lines occurring from these conduction carriers can be ascribed to relaxation involving the spin-orbit coupling[23,24] in iodine atoms. The bromine doping of *E* and *G* increases the pristine $\Delta H_{\text{p.p.}}$ to $\frac{1}{4}-\frac{1}{3}$ of those of I_2-*E* and I_2-*G*.[22] These broadenings strongly suggest that the conduction carriers have a finite probability of existing on the dopant species, that is, they are not necessarily confined to the metallic islands. Although a Z^4 dependence of the ESR line shape on the dopant atoms (*Z* is the atomic number) is expected from a simple extension of the discussion in Ref. 24, the present polyacenic samples show different *Z* dependences in each sample. Namely, from the experimental data obtained for iodine- and bromine-doped samples,[22] $\Delta H_{\text{p.p.}}$ of the *E* and *G* series seems to follow a Z^{α} law, with $\alpha=2.92\pm0.09$ and $\alpha=3.21\pm0.21$, respectively. It is also interesting to note the *g* values of the ESR peaks of I_2-*D*, I_2-*E*, and I_2-*G* are large, similar to that of I_2^- anion radicals, 2.1561.[25]

Similar effects of the spin-orbit coupling were reported for graphite intercalated with GeF_4, AsF_5, SbF_5, and IF_5.[26] In heavily iodine-doped polyacetylene, the ESR signal even disappears, which was attributed to an extreme broadening of the line due to spin-orbit coupling.[14,21] A large ESR linewidth was also observed in organic radical crystals such as Würster's blue iodide (*N,N,N',N'*-tetramethyl-*p*-diaminobenzene iodide) which gave $\Delta H_{\text{p.p}}=62.0$ G.[27]

Narrowing of the line as observed at $-100\,^{\circ}$C for all except I_2-*A*1 is explicable by either a Korringa-type mechanism (see Sec. III A) or suppression of conduction-carrier hopping from the metallic islands to the dopant species.

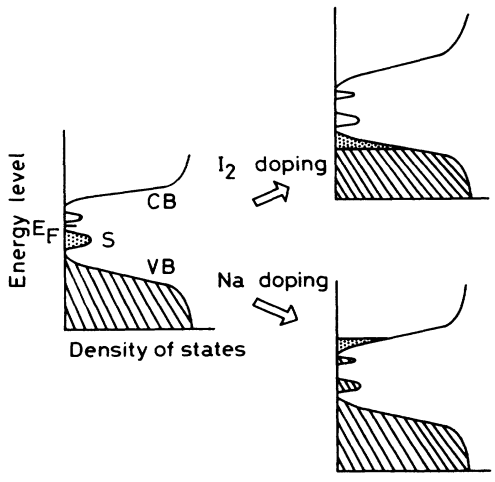

FIG. 4. Schematic representation of the Fermi level (E_F) area of the pristine samples (left) and those of the heavily-doped samples with iodine and sodium (right). VB, CB, and S denote the valence and the conduction bands, and the impurity level accommodating unpaired electrons, respectively. Dotted area accommodates unpaired electrons and shaded area paired electrons.

C. Sodium-doped samples

Polyacenic samples heavily doped with sodium also show a slight broadening of the line as seen in Fig. 2(c) and Table III, which is remarkable in Na-*D*, Na-*E*, and Na-*G*. It has been claimed that Na-*D* already shows an *n*-type metallic thermoelectric power.[28] Hence it is again highly possible that the linewidth of these three is influenced by the spin-orbit coupling at the sodium atoms. Since the spin-orbit coupling constant of sodium is not as large as iodine's,[29] the degree of the broadening is much smaller as compared with the iodine-doped case. Nevertheless, it is not legitimate to ignore the possibility that the conduction carriers partially stay on sodium atoms. This trend is suppressed at lower temperatures as is evident from the narrowing of the line of Na-*D*, Na-*E*, and Na-*G* at $-100\,^{\circ}$C. A similar spin-orbit coupling effect was observed in polyacetylene doped with alkali metals.[30] The *g* values of Na-doped samples are not much different from those of the pristine samples. Alkali-metal- (Li and K) doped graphite powder also shows *g* values from 2.0026 to 2.0028,[31] whereas $g_{\parallel}$ and $g_{\perp}$ (with respect to the *ab* plane) of pristine graphite are equal to 2.0026 and 2.0495, respectively.[15]

The spin concentrations of the Na-doped samples are slightly less than those of the pristine samples and remarkably less in Na-*D*. These tendencies agree well with the results of magnetic susceptibility measurements of the Na-doped samples.[32] Hence it is possible to conclude that the defect-oriented unpaired electrons in the impurity levels of the pristine samples are annihilated by donation of another electron from sodium. In the heavily-doped state more conduction electrons are generated by sodium near the bottom of the conduction band as illustrated in Fig. 4.

IV. CONCLUDING REMARKS

ESR studies were performed for pristine and heavily-doped polyacenic materials prepared by pyrolytic treatment of PF resin under various temperatures (T_p). There

are five major findings in the present investigation.

(1) The ESR linewidth and the spin concentration of the pristine sample varies with T_p. The sample with $T_p = 680\,^{\circ}\mathrm{C}$ shows the minimum linewidth and the maximum spin concentration. These reflect the structural characteristics of each pristine sample.

(2) At the initial stage of the doping by both I_2 or Na, it is highly possible that defect-oriented spins are scavenged resulting in a decrease of the spin concentration.

(3) Further doping from the above stage generates conduction carriers near the top of the valence band or the bottom of the conduction band.

(4) The ESR line of the heavily doped samples, particularly those with higher T_p's, becomes broader. This suggests that the conduction electrons are influenced by the spin-orbit coupling in the dopant species. In other words, the conduction electrons exist on the dopant with a finite probability.

(5) The itineration of the conduction electrons on the dopant is suppressed at lower temperatures.

These findings in the ESR spectroscopic studies of polyacenic materials offer information not only on their magnetic properties but also on their structural variation and conduction mechanisms. It is desirable to systematically check the spin-orbit coupling mechanism as well as other relaxation process in these polyacenic materials with a series of dopant species. This study is currently underway and will be reported in the near future.

ACKNOWLEDGMENTS

This work was partially supported by a Grant-in-Aid for Scientific Research from the Ministry of Education, Science and Culture of Japan. One of the authors (K.T.) acknowledges the receipt of financial support from the Kawakami Memorial Foundation.

[1]H. Honda, K. Ouchi, and S. Toyoda, J. Chem. Soc. Jpn. **76**, 368 (1955).
[2]W. Bücker, J. Non-Cryst. Solids **12**, 115 (1973).
[3]H. B. Brom, Y. Tomkiewicz, A. Aviram, A. Broers, and B. Sunners, Solid State Commun. **35**, 135 (1980).
[4]M. Murakami, H. Yasujima, Y. Yumoto, S. Mizogami, and S. Yoshimura, Solid State Commun. **45**, 1085 (1983).
[5]H. Teoh, P. D. Metz, and W. G. Wilhelm, Mol. Cryst. Liq. Cryst. **83**, 297 (1982), and references therein.
[6]C. Jackson and W. F. K. Wynne-Jones, Carbon **2**, 227 (1964).
[7]T. Yamabe, K. Tanaka, K. Ohzeki, and S. Yata, J. Phys. (Paris) Colloq. **44**, C3-645 (1983); K. Tanaka, K. Ohzeki, T. Yamabe, and S. Yata, Synth. Met. **9**, 41 (1984).
[8]S. Yata, Y. Hato, K. Sakurai, T. Osaki, K. Tanaka, and T. Yamabe, Synth. Met. **18**, 645 (1987).
[9]K. Tanaka, S. Yamanaka, T. Koike, T. Yamabe, K. Yoshino, G. Ishii, and S. Yata, Phys. Rev. B **32**, 6675 (1985).
[10]K. Tanaka, M. Ueda, T. Yamabe, and S. Yata, Polym. Prep. Jpn. **33**, 2475 (1984).
[11]K. Tanaka, K. Yoshizawa, T. Koike, T. Yamabe, J. Yamauchi, Y. Deguchi, and S. Yata, Solid State Commun. **52**, 343 (1984).
[12]Although the term "band" is only meaningful in the crystalline material, we use this for the sake of simplicity mainly with respect to the metallic-island structure throughout this article.
[13]See, S. Yata (Kanebo Ltd.), European Patent, No. 0067444; United States Patent, No. 4601849.
[14]J. C. W. Chien, G. E. Wnek, F. E. Karasz, J. M. Warakomski, L. C. Dickinson, A. J. Heeger, and A. G. MacDiarmid, Macromolecules **15**, 614 (1982).
[15]G. Wagoner, Phys. Rev. **118**, 647 (1960).
[16]S. Toyoda, Rep. Resources Research Inst. Jpn. **74**, 1 (1969).
[17]F. J. Dyson, Phys. Rev. **98**, 349 (1955).
[18]I. C. Lewis, Carbon **20**, 519 (1982).
[19]I. B. Goldberg, H. R. Crowe, P. R. Newman, A. J. Heeger, and A. G. MacDiarmid, J. Chem. Phys. **70**, 1132 (1979).
[20]J. Korringa, Physica (The Hague), **16**, 601 (1950).
[21]D. Davidov, S. Roth, W. Neumann, and H. Sixl, Solid State Commun. **52**, 375 (1984).
[22]K. Tanaka, T. Koike, H. Nishino, T. Yamabe, J. Yamauchi, Y. Deguchi, and S. Yata, Synth. Met. **18**, 521 (1987).
[23]R. J. Elliott, Phys. Rev. **96**, 266 (1954).
[24]Y. Yafet, Solid State Phys. **14**, 1 (1963).
[25]*Magnetic Properties of Free Radicals,* Group 2/Vol. 1 of *Landolt-Börnstein,* edited by H. Fischer and K.-H. Hellwege (Springer, Berlin, 1965); *ibid.*, Group 2/Vol. 9a (1977) (Vol. 9a is a supplement to Vol. 1).
[26]R. Davidov, O. Milo, I. Palchan, and H. Selig, Synth. Met. **8**, 83 (1983).
[27]J. Yamauchi, H. Fujita, and Y. Deguchi, in *Proceedings of the Symposium of Molecular Structure, Sapporo, Japan, 1977* (Association for Molecular Science, Sapporo, 1977), p. 182.
[28]H. Ueno, G. Ishii, K. Yoshino, K. Tanaka, T. Yamabe, and S. Yata, Synth. Met. **18**, 515 (1987).
[29]See, for example, A. Carrington and A. D. McLachlan, *Introduction to Magnetic Resonance* (Harper & Row, New York, 1967), Chap. 9.
[30]F. Rachdi and P. Bernier, Phys. Rev. B **33**, 7817 (1986).
[31]P. Lauginie, H. Estrade, J. Conrad, D. Guerard, P. Lagrange, M. El Makrini, Physica **99B**, 514 (1980).
[32]K. Tanaka, T. Koike, M. Ando, T. Yamabe, J. Yamauchi, Y. Deguchi, and S. Yata, Polym. Prep. Jpn. **34**, 523 (1985).